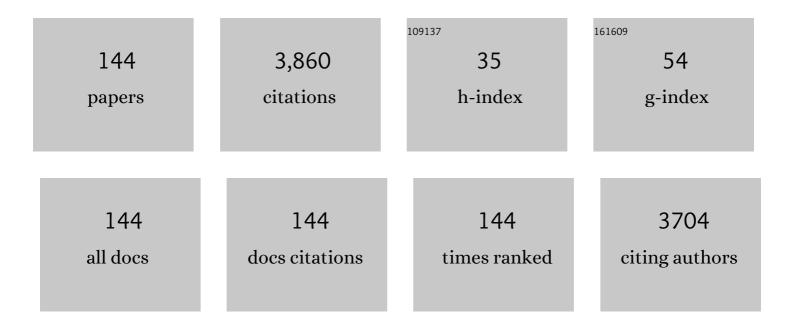
Raul Gago

List of Publications by Year in descending order

Source: https://exaly.com/author-pdf/9282897/publications.pdf Version: 2024-02-01



RALLI CACC

#	Article	IF	CITATIONS
1	Production of ordered silicon nanocrystals by low-energy ion sputtering. Applied Physics Letters, 2001, 78, 3316-3318.	1.5	226
2	Self-Organized Ordering of Nanostructures Produced by Ion-Beam Sputtering. Physical Review Letters, 2005, 94, 016102.	2.9	212
3	Self-organized nanopatterning of silicon surfaces by ion beam sputtering. Materials Science and Engineering Reports, 2014, 86, 1-44.	14.8	142
4	Stress-induced solid flow drives surface nanopatterning of silicon by ion-beam irradiation. Physical Review B, 2012, 86, .	1.1	92
5	Structure and properties of silver-containing a-C(H) films deposited by plasma immersion ion implantation. Surface and Coatings Technology, 2008, 202, 3675-3682.	2.2	87
6	Towards nanometric resolution in multilayer depth profiling: a comparative study of RBS, SIMS, XPS and GDOES. Analytical and Bioanalytical Chemistry, 2010, 396, 2725-2740.	1.9	79
7	Electrochemical behavior of nanocrystalline Ta/TaN multilayer on 316L stainless steel: Novel bipolar plates for proton exchange membrane fuel-cells. Journal of Power Sources, 2016, 322, 1-9.	4.0	74
8	Hydrogen quantification in hydrogenated amorphous carbon films by infrared, Raman, and x-ray absorption near edge spectroscopies. Journal of Applied Physics, 2009, 105, .	1.1	73
9	Sixfold ring clustering insp2-dominated carbon and carbon nitride thin films: A Raman spectroscopy study. Physical Review B, 2006, 73, .	1.1	70
10	Spectroscopy of π bonding in hard graphitic carbon nitride films: Superstructure of basal planes and hardening mechanisms. Physical Review B, 2000, 62, 4261-4264.	1.1	68
11	Structural properties and corrosion resistance of tantalum nitride coatings produced by reactive DC magnetron sputtering. RSC Advances, 2016, 6, 89061-89072.	1.7	65
12	Temperature influence on the production of nanodot patterns by ion beam sputtering of Si(001). Physical Review B, 2006, 73, .	1.1	64
13	Tuning the surface morphology in self-organized ion beam nanopatterning of Si(001) via metal incorporation: from holes to dots. Nanotechnology, 2008, 19, 355306.	1.3	63
14	Nanopatterning of silicon surfaces by low-energy ion-beam sputtering: dependence on the angle of ion incidence. Nanotechnology, 2002, 13, 304-308.	1.3	61
15	Evolution ofsp2networks with substrate temperature in amorphous carbon films: Experiment and theory. Physical Review B, 2005, 72, .	1.1	61
16	Bonding and hardness in nonhydrogenated carbon films with moderate sp3 content. Journal of Applied Physics, 2000, 87, 8174-8180.	1.1	57
17	Characterization of the unoccupied and partially occupied states of TTF-TCNQ by XANES and first-principles calculations. Physical Review B, 2003, 68, .	1.1	54
18	Observation and Modeling of Interrupted Pattern Coarsening: Surface Nanostructuring by Ion Erosion. Physical Review Letters, 2010, 104, 026101.	2.9	54

#	Article	IF	CITATIONS
19	Order enhancement and coarsening of self-organized silicon nanodot patterns induced by ion-beam sputtering. Applied Physics Letters, 2006, 89, 233101.	1.5	53
20	Comparative depth-profiling analysis of nanometer-metal multilayers by ion-probing techniques. TrAC - Trends in Analytical Chemistry, 2009, 28, 494-505.	5.8	51
21	Identification of ternary boron–carbon–nitrogen hexagonal phases by x-ray absorption spectroscopy. Applied Physics Letters, 2001, 78, 3430-3432.	1.5	50
22	Diagnostics of a N2/Ar direct current magnetron discharge for reactive sputter deposition of fullerene-like carbon nitride thin films. Journal of Applied Physics, 2003, 94, 7059-7066.	1.1	49
23	Nanoscale pattern formation at surfaces under ion-beam sputtering: A perspective from continuum models. Nuclear Instruments & Methods in Physics Research B, 2011, 269, 894-900.	0.6	49
24	Self-Organized Surface Nanopatterning by Ion Beam Sputtering. , 2009, , 323-398.		46
25	Nonuniversality due to inhomogeneous stress in semiconductor surface nanopatterning by low-energy ion-beam irradiation. Physical Review B, 2015, 91, .	1.1	44
26	Transition from amorphous boron carbide to hexagonal boron carbon nitride thin films induced by nitrogen ion assistance. Journal of Applied Physics, 2002, 92, 5177-5182.	1.1	43
27	Detecting with X-ray absorption spectroscopy the modifications of the bonding structure of graphitic carbon by amorphisation, hydrogenation and nitrogenation. Surface Science, 2001, 482-485, 530-536.	0.8	42
28	Direct Nanopatterning of Metal Surfaces Using Self-Assembled Molecular Films. Advanced Materials, 2004, 16, 405-409.	11.1	42
29	Boron carbides formed by coevaporation of B and C atoms: Vapor reactivity, <mml:math xmlns:mml="http://www.w3.org/1998/Math/MathML" display="inline"> <mml:mrow> <mml:msub> <mml:mi mathvariant="normal">B <mml:mi> </mml:mi> </mml:mi </mml:msub> <mml:msub> <mml:mi mathvariant="normal">C <mml:mrow> <mml:mn>1</mml:mn> <mml:mo> â^² </mml:mo> <mml:mi>x<td>1.1 nml:mi> <td>42 nml:mrow><!--1</td--></td></td></mml:mi></mml:mrow></mml:mi </mml:msub></mml:mrow></mml:math 	1.1 nml:mi> <td>42 nml:mrow><!--1</td--></td>	42 nml:mrow> 1</td
30	and bonding structure. Physical Review 6, 2006, 77, . X-Ray absorption studies of cubic boron–carbon–nitrogen films grown by ion beam assisted evaporation. Diamond and Related Materials, 2001, 10, 1165-1169.	1.8	40
31	Correlation between bonding structure and microstructure in fullerenelike carbon nitride thin films. Physical Review B, 2005, 71, .	1.1	40
32	Tribological properties of ternary BCN films with controlled composition and bonding structure. Diamond and Related Materials, 2004, 13, 1532-1537.	1.8	39
33	Spectroscopic ellipsometry investigation of amorphous carbon films with different sp3 content: relation with protein adsorption. Thin Solid Films, 2004, 455-456, 530-534.	0.8	37
34	Nanopatterning dynamics on Si(100) during oblique 40-keV Ar <mml:math xmlns:mml="http://www.w3.org/1998/Math/MathML" display="inline"><mml:msup><mml:mrow /><mml:mo>+</mml:mo></mml:mrow </mml:msup>erosion with metal codeposition: Morphological and compositional correlation. Physical Review B, 2012, 86, .</mml:math 	1.1	37
35	Growth and characterisation of boron–carbon–nitrogen coatings obtained by ion beam assisted evaporation. Vacuum, 2002, 64, 199-204.	1.6	36
36	Tribological study of hydrogenated amorphous carbon films with tailored microstructure and composition produced by bias-enhanced plasma chemical vapour deposition. Diamond and Related Materials, 2010, 19, 1093-1102.	1.8	36

Raul Gago

#	Article	IF	CITATIONS
37	Hardening Mechanisms in Graphitic Carbon Nitride Films Grown with N2/Ar Ion Assistance. Chemistry of Materials, 2001, 13, 129-135.	3.2	35
38	Early stage of ripple formation on Ge(001) surfaces under near-normal ion beam sputtering. Nanotechnology, 2008, 19, 035304.	1.3	35
39	Spectral evidence of spinodal decomposition, phase transformation and molecular nitrogen formation in supersaturated TiAlN films upon annealing. Acta Materialia, 2011, 59, 6287-6296.	3.8	35
40	Direct spectroscopic evidence of self-formed C60 inclusions in fullerenelike hydrogenated carbon films. Applied Physics Letters, 2008, 92, .	1.5	34
41	Production of nanohole/nanodot patterns on Si(001) by ion beam sputtering with simultaneous metal incorporation. Journal of Physics Condensed Matter, 2009, 21, 224009.	0.7	34
42	Thin Films of Molecular Metals TTF-TCNQ. Journal of Solid State Chemistry, 2002, 168, 384-389.	1.4	33
43	Depth-resolved analysis of spontaneous phase separation in the growth of lattice-matched AlInN. Journal Physics D: Applied Physics, 2010, 43, 055406.	1.3	33
44	Effect of the substrate temperature on the deposition of hydrogenated amorphous carbon by PACVD at 35 kHz. Thin Solid Films, 1999, 338, 88-92.	0.8	32
45	Deposition of TiN/AIN bilayers on a rotating substrate by reactive sputtering. Surface and Coatings Technology, 2002, 157, 26-33.	2.2	32
46	Electronic structure and conductivity of nanocomposite metal (Au, Ag, Cu, Mo)-containing amorphous carbon films. Solid State Sciences, 2009, 11, 1742-1746.	1.5	32
47	Establishing the mechanism of thermally induced degradation of ZnO:Al electrical properties using synchrotron radiation. Applied Physics Letters, 2010, 96, 141907.	1.5	32
48	X-Ray absorption studies of bonding environments in graphitic carbon nitride. Diamond and Related Materials, 2001, 10, 1170-1174.	1.8	30
49	In-depth optical and structural study of silver-based low-emissivity multilayer coatings for energy-saving applications. Journal Physics D: Applied Physics, 2004, 37, 1554-1557.	1.3	29
50	<i>In situ</i> x-ray scattering study of self-organized nanodot pattern formation on GaSb(001) by ion beam sputtering. Applied Physics Letters, 2007, 91, .	1.5	29
51	Boron–carbon–nitrogen compounds grown by ion beam assisted evaporation. Thin Solid Films, 2000, 373, 277-281.	0.8	28
52	Universal non-equilibrium phenomena at submicrometric surfaces and interfaces. European Physical Journal: Special Topics, 2007, 146, 427-441.	1.2	28
53	Surface nanopatterns induced by ion-beam sputtering. Journal of Physics Condensed Matter, 2009, 21, 220301.	0.7	28
54	Fine structure at the X-ray absorption π* and σ* bands of amorphous carbon. Diamond and Related Materials. 2003. 12. 110-115.	1.8	27

#	Article	IF	CITATIONS
55	Molding and Replication of Ceramic Surfaces with Nanoscale Resolution. Small, 2005, 1, 300-309.	5.2	27
56	Bonding structure of BCN nanopowders prepared by ball milling. Diamond and Related Materials, 2007, 16, 1450-1454.	1.8	27
57	X-ray absorption near-edge structure of hexagonal ternary phases in sputter-deposited TiAlN films. Journal of Alloys and Compounds, 2013, 561, 87-94.	2.8	26
58	Surface nanopatterning of metal thin films by physical vapour deposition onto surface-modified silicon nanodots. Nanotechnology, 2004, 15, S197-S200.	1.3	24
59	Hemocompatibility of low-friction boron–carbon–nitrogen containing coatings. Journal of Biomedical Materials Research - Part B Applied Biomaterials, 2006, 77B, 179-187.	1.6	24
60	Hydrogen stability in hydrogenated amorphous carbon films with polymer-like and diamond-like structure. Journal of Applied Physics, 2012, 112, .	1.1	24
61	Fullerenelike arrangements in carbon nitride thin films grown by direct ion beam sputtering. Applied Physics Letters, 2005, 87, 071901.	1.5	23
62	Optical and compositional analysis of functional SiOxCy:H coatings on polymers. Thin Solid Films, 2006, 515, 2493-2496.	0.8	23
63	X-ray Spectroscopic and Magnetic Investigation of C:Ni Nanocomposite Films Grown by Ion Beam Cosputtering. Journal of Physical Chemistry C, 2008, 112, 12628-12637.	1.5	23
64	Aluminum incorporation in Ti1â^'xAlxN films studied by x-ray absorption near-edge structure. Journal of Applied Physics, 2009, 105, .	1.1	22
65	Independence of interrupted coarsening on initial system order: ion-beam nanopatterning of amorphous versus crystalline silicon targets. Journal of Physics Condensed Matter, 2012, 24, 375302.	0.7	22
66	Effect of Carbon Incorporation on the Microstructure of BC _{<i>x</i>} N (<i>x</i> = 0.25, 1,) Tj ETQq0 2010, 22, 1949-1951.	0 0 rgBT / 3.2	Overlock 10 ⁻ 21
67	Phase composition and tribomechanical properties of Ti–B–C nanocomposite coatings prepared by magnetron sputtering. Journal Physics D: Applied Physics, 2012, 45, 375401.	1.3	21
68	The effect of nitrogen incorporation on the bonding structure of hydrogenated carbon nitride films. Journal of Applied Physics, 2007, 101, 063515.	1.1	19
69	Surface Morphology of Heterogeneous Nanocrystalline Rutile/Amorphous Anatase TiO ₂ Films Grown by Reactive Pulsed Magnetron Sputtering. Plasma Processes and Polymers, 2010, 7, 813-823.	1.6	19
70	Development of interference filters based on multilayer porous silicon structures. Materials Science and Engineering C, 2003, 23, 1043-1046.	3.8	17
71	Spectroscopic evidence of NOx formation and band-gap narrowing in N-doped TiO2 films grown by pulsed magnetron sputtering. Materials Chemistry and Physics, 2012, 136, 729-736.	2.0	17
72	Bonding structure and morphology of chromium oxide films grown by pulsed-DC reactive magnetron sputter deposition. Journal of Alloys and Compounds, 2016, 672, 529-535.	2.8	17

#	Article	IF	CITATIONS
73	Stress measurement and stress relaxation during magnetron sputter deposition of cubic boron nitride thin films. Thin Solid Films, 2004, 447-448, 131-135.	0.8	16
74	Effect of the growth temperature and the AlN mole fraction on In incorporation and properties of quaternary III-nitride layers grown by molecular beam epitaxy. Journal of Applied Physics, 2008, 104, 083510.	1.1	16
75	A review of monolithic and multilayer coatings within the boron–carbon–nitrogen system by ion-beam-assisted deposition. Journal of Materials Research, 2012, 27, 743-764.	1.2	16
76	Synthesis of carbon nitride thin films by low-energy ion beam assisted evaporation: on the mechanisms for fullerene-like microstructure formation. Thin Solid Films, 2005, 483, 89-94.	0.8	15
77	Nanometric resolution in glow discharge optical emission spectroscopy and Rutherford backscattering spectrometry depth profiling of metal (Cr, Al) nitride multilayers. Spectrochimica Acta, Part B: Atomic Spectroscopy, 2006, 61, 545-553.	1.5	15
78	Calibration of nitrogen content for GDOES depth profiling of complex nitride coatings. Journal of Analytical Atomic Spectrometry, 2007, 22, 1512.	1.6	15
79	Transition from smoothing to roughening of ion-eroded GaSb surfaces. Applied Physics Letters, 2009, 94, 193103.	1.5	15
80	On the bonding structure of hydrogenated carbon nitrides grown by electron cyclotron resonance chemical vapour deposition: towards the synthesis of non-graphitic carbon nitrides. Diamond and Related Materials, 2002, 11, 1161-1165.	1.8	14
81	Direct molding of nanopatterned polymeric films: Resolution and errors. Applied Physics Letters, 2003, 82, 457-459.	1.5	13
82	X-ray diffraction study of stress relaxation in cubic boron nitride films grown with simultaneous medium-energy ion bombardment. Applied Physics Letters, 2004, 85, 5905-5907.	1.5	13
83	Characterization of biofunctional thin films deposited by activated vapor silanization. Journal of Materials Research, 2008, 23, 1931-1939.	1.2	13
84	Photoluminescence enhancement in quaternary III-nitrides alloys grown by molecular beam epitaxy with increasing Al content. Journal of Applied Physics, 2008, 103, 046104.	1.1	13
85	lon damage overrides structural disorder in silicon surface nanopatterning by low-energy ion beam sputtering. Europhysics Letters, 2015, 109, 48003.	0.7	13
86	Aluminium incorporation in AlxGa1â´'xN/GaN heterostructures: A comparative study by ion beam analysis and X-ray diffraction. Thin Solid Films, 2008, 516, 8447-8452.	0.8	12
87	Thermal Stability and Oxidation Resistance of Nanocomposite TiC/a Protective Coatings. Plasma Processes and Polymers, 2009, 6, S462.	1.6	12
88	Ultrasmooth growth of amorphous silicon films through ion-induced long-range surface correlations. Applied Physics Letters, 2011, 98, 011904.	1.5	12
89	Influence of metal co-deposition on silicon nanodot patterning dynamics during ion-beam sputtering. Nanotechnology, 2014, 25, 415301.	1.3	12
90	Strong Room Temperature Blue Emission from Rapid Thermal Annealed Cerium-Doped Aluminum (Oxy)Nitride Thin Films. ACS Photonics, 2017, 4, 1945-1953.	3.2	12

#	Article	IF	CITATIONS
91	Heavy-ion ERDA and spectroscopic ellipsometry characterization of a SiOC:H layered structure as functional coating on polymeric lenses. Nuclear Instruments & Methods in Physics Research B, 2004, 219-220, 908-913.	0.6	11
92	Detection of intrinsic stress in cubic boron nitride films by x-ray absorption near-edge structure: Stress relaxation mechanisms by simultaneous ion implantation during growth. Physical Review B, 2007, 76, .	1.1	11
93	Versatile vacuum chamber for <i>in situ</i> surface X-ray scattering studies. Journal of Synchrotron Radiation, 2008, 15, 414-419.	1.0	11
94	Annealing of heterogeneous phase TiO2 films: An X-ray absorption and morphological study. Chemical Physics Letters, 2011, 511, 367-371.	1.2	11
95	Growth of nanocolumnar thin films on patterned substrates at oblique angles. Plasma Processes and Polymers, 2019, 16, 1800135.	1.6	11
96	Identification of Ternary Phases in TiBC/a Nanocomposite Thin Films: Influence on the Electrical and Optical Properties. Plasma Processes and Polymers, 2011, 8, 579-588.	1.6	10
97	Surface morphology of molybdenum silicide films upon low-energy ion beam sputtering. Journal of Physics Condensed Matter, 2018, 30, 264003.	0.7	10
98	X-Ray absorption study of the bonding structure of BCN compounds enriched in carbon by CH4 ion assistance. Diamond and Related Materials, 2002, 11, 1295-1299.	1.8	9
99	Impact of Annealing on the Conductivity of Amorphous Carbon Films Incorporating Copper and Gold Nanoparticles Deposited by Pulsed Dual Cathodic Arc. Plasma Processes and Polymers, 2009, 6, S438.	1.6	9
100	Sublattice-specific ordering of ZnO layers during the heteroepitaxial growth at different temperatures. Journal of Applied Physics, 2011, 110, 113516.	1.1	9
101	Self-organized surface nanopatterns on Cd(Zn)Te crystals induced by medium-energy ion beam sputtering. Journal Physics D: Applied Physics, 2013, 46, 455302.	1.3	9
102	Influence of electronic structure, plasmon-phonon and plasmon-polariton excitations on anomalously low heat conductivity in TiAlN/Ag nanoscale multilayer coatings. Current Applied Physics, 2016, 16, 459-468.	1.1	9
103	Structure of MgO/V/MgO(001) thin films studied by the combination of X-ray photoemission and ion beam analysis techniques. Surface Science, 2006, 600, 497-506.	0.8	8
104	Interface-Induced Plasmon Nonhomogeneity in Nanostructured Metal-Dielectric Planar Metamaterial. Journal of Nanomaterials, 2015, 2015, 1-9.	1.5	8
105	Choice of boron–carbon–nitrogen coating material for electron emission based on photoelectric yield measurements during x-ray absorption studies. Journal of Vacuum Science & Technology an Official Journal of the American Vacuum Society B, Microelectronics Processing and Phenomena, 2001, 19. 1358.	1.6	7
106	Hybrid titania–aminosilane platforms evaluated with human mesenchymal stem cells. Journal of Biomedical Materials Research - Part B Applied Biomaterials, 2007, 83B, 232-239.	1.6	7
107	Structural impact of chromium incorporation in as-grown and flash-lamp-annealed sputter deposited titanium oxide films. Journal of Alloys and Compounds, 2017, 729, 438-445.	2.8	7
108	Chemical Functionalization of the Zinc Selenide Surface and Its Impact on Lactobacillus rhamnosus GG Biofilms. ACS Applied Materials & Interfaces, 2020, 12, 14933-14945.	4.0	7

#	Article	IF	CITATIONS
109	Nitrogen incorporation in carbon nitride films produced by direct and dual ion-beam sputtering. Journal of Applied Physics, 2005, 98, 074907.	1.1	6
110	Influence of steering effects on strain detection in AlGaInN/GaN heterostructures by ion channelling. Journal Physics D: Applied Physics, 2009, 42, 065420.	1.3	6
111	Highly ordered silicide ripple patterns induced by medium-energy ion irradiation. Physical Review B, 2020, 102, .	1.1	6
112	Thin Film Growth by Ion-Beam-Assisted Deposition Techniques. , 2006, , 345-382.		6
113	Influence of ion current on the growth of carbon films by ion-beam-assisted deposition. Diamond and Related Materials, 1999, 8, 1944-1950.	1.8	5
114	Rutherford backscattering spectrometry characterization of nanoporous chalcogenide thin films grown at oblique angles. Journal of Analytical Atomic Spectrometry, 2008, 23, 981.	1.6	5
115	Breakdown of anomalous channeling with ion energy for accurate strain determination in GaN-based heterostructures. Applied Physics Letters, 2009, 95, 051921.	1.5	5
116	Mg doping of InGaN layers grown by PA-MBE for the fabrication of Schottky barrier photodiodes. Journal Physics D: Applied Physics, 2010, 43, 335101.	1.3	5
117	Atomistic model of ultra-smooth amorphous thin film growth by low-energy ion-assisted physical vapour deposition. Journal Physics D: Applied Physics, 2013, 46, 395303.	1.3	5
118	Hydrogen incorporation in CNx films deposited by ECR chemical vapor deposition. Diamond and Related Materials, 2003, 12, 632-635.	1.8	4
119	Microanalysis of Ar and He bombarded biomedical polymer films. Nuclear Instruments & Methods in Physics Research B, 2007, 257, 496-500.	0.6	4
120	High-resolution hydrogen profiling in AlGaN/GaN heterostructures grown by different epitaxial methods. Journal Physics D: Applied Physics, 2009, 42, 055406.	1.3	4
121	Extended X-ray absorption fine structure (EXAFS) investigations of Ti bonding environment in sputter-deposited nanocomposite TiBC/a-C thin films. IOP Conference Series: Materials Science and Engineering, 2010, 12, 012012.	0.3	4
122	Optimized allylamine deposition for improved pluripotential cell culture. Vacuum, 2011, 85, 1071-1075.	1.6	4
123	The confinement of phonon propagation in TiAlN/Ag multilayer coatings with anomalously low heat conductivity. Applied Physics Letters, 2016, 108, .	1.5	4
124	Correlated effects of fluorine and hydrogen in fluorinated tin oxide (FTO) transparent electrodes deposited by sputtering at room temperature. Applied Surface Science, 2021, 537, 147906.	3.1	4
125	Soft X-ray absorption study of sputtered tin oxide films. Journal of Alloys and Compounds, 2022, 902, 163768.	2.8	4
126	Damage effects from medium-energy ion bombardment during the growth of cubic-boron nitride films. Journal of Vacuum Science and Technology A: Vacuum, Surfaces and Films, 2003, 21, 1739-1744.	0.9	3

#	Article	IF	CITATIONS
127	Smart modification of magnetron sputtered TiN surfaces for stimulated differentiation. Surface and Coatings Technology, 2008, 203, 905-908.	2.2	3
128	Features of electronic and lattice mechanisms of transboundary heat transfer in multilayer nanolaminate TiAlN/Ag coatings. Scientific Reports, 2017, 7, 17078.	1.6	3
129	Phase Selectivity in Cr and N Co-Doped TiO2 Films by Modulated Sputter Growth and Post-Deposition Flash-Lamp-Annealing. Coatings, 2019, 9, 448.	1.2	3
130	Structural and chemical characterization of functional SiO[sub x]C[sub y]:H coatings for polymeric lenses. Journal of Vacuum Science & Technology an Official Journal of the American Vacuum Society B, Microelectronics Processing and Phenomena, 2004, 22, 2402.	1.6	2
131	Interplay between Morphology and Surface Transport in Nanopatterns Produced by Ion-Beam Sputtering. Materials Research Society Symposia Proceedings, 2007, 1059, 1.	0.1	2
132	Surface morphology of amorphous SiO ₂ substrates bombarded with 1.0 MeV Si ⁺ ions. Journal of Physics Condensed Matter, 2018, 30, 274005.	0.7	2
133	Ultraviolet optical excitation of near infrared emission of Yb-doped crystalline aluminum oxynitride thin films. Journal of Applied Physics, 2018, 124, 033102.	1.1	2
134	Soft X-ray absorption study of tantalum incorporation in titanium oxide films: Impact of flash-lamp annealing. Ceramics International, 2020, 46, 15772-15778.	2.3	2
135	Study of SiN _x :H _y passivant layers for AlGaN/GaN high electron mobility transistors. Physica Status Solidi C: Current Topics in Solid State Physics, 2008, 5, 518-521.	0.8	1
136	Energy dependence of the ripple wavelength for ion-beam sputtering of silicon: Experiments and theory. , 2013, , .		1
137	Special issue on surfaces patterned by ion sputtering. Journal of Physics Condensed Matter, 2018, 30, 450301.	0.7	1
138	Interconnections between Electronic Structure and Optical Properties of Multilayer Nanolaminate TiAlN/Ag and Al2O3/Ag Coatings. Coatings, 2018, 8, 290.	1.2	1
139	In Situ Monitoring of Alkanethiol Selfâ€Assembly onto Zinc Selenide: The Role of Substrate Pretreatment and Its Implication in Bacterial Attachment. Advanced Materials Interfaces, 2020, 7, 2000848.	1.9	1
140	Morphological impact of low-energy Xe ⁺ irradiation on polycrystalline titanium targets. Journal of Physics: Conference Series, 2020, 1593, 012041.	0.3	1
141	Plasma Process. Polym. 9â \in 10/2010. Plasma Processes and Polymers, 2010, 7, .	1.6	0
142	Ultraviolet to infrared downshifting in Ce and Yb co-doped aluminum oxynitride thin films. Journal Physics D: Applied Physics, 2019, 52, 285105.	1.3	0
143	Anomalous Heat Transport in Nanolaminate Metal/Oxide Multilayer Coatings: Plasmon and Phonon Excitations. Coatings, 2020, 10, 260.	1.2	0
144	Efecto del argon en pelÃculas CN _x H _y depositadas mediante ECR-CVD. Boletin De La Sociedad Espanola De Ceramica Y Vidrio, 2004, 43, 491-493.	0.9	0